Available online at www.sciencedirect.com
ScienceDirect
Polymer 47 (2006) 6328–6336
polymer
www.elsevier.com/locate/polymer

Thermal and crystallisation behaviours of blends of polyamide 12 with styrene–ethylene/butylene–styrene rubbers

Seno Jose [a], P. Selvin Thomas [a], Sabu Thomas [a,*], J. Karger-Kocsis [b]

[a] *School of Chemical Sciences, Mahatma Gandhi University, Priyadarshini Hills P.O., Kottayam, Kerala 686 560, India*
[b] *Institute of Composite Materials Ltd, University of Kaiserslautern, P.O. Box 3049, D-67653 Kaiserslautern, Germany*

Received 26 November 2005; received in revised form 9 June 2006; accepted 4 July 2006
Available online 1 August 2006

Abstract

Polyamide 12 (PA12)/styrene–ethylene/butylene–styrene (SEBS) and PA12/maleic anhydride grafted SEBS (SEBS-*g*-MA) blends were prepared in a twin-screw extruder followed by injection moulding. Thermal and crystallisation behaviours of these blends were evaluated. Thermal properties and morphology of the blends were estimated using thermo gravimetric analysis (TGA) and scanning electron microscopy (SEM), respectively. The phase structure of the blends was interpreted by dynamic mechanical thermal analyser (DMTA). In terms of temperature at maximum rate of degradation (T_{max}) and integral procedural decomposition temperature (IPDT), it was found that PA12/SEBS-*g*-MA (PM) blends possessed greater thermal stability than PA12/SEBS (PS) blends. The kinetics of degradation process of PA12 and its blends were studied using Coats–Redfern (CR) method. It was found that there is no appreciable change in the thermal stability of PA12 in the presence of small amount of rubber phase. A good correlation was observed between the thermal properties and phase morphology of the blends. Melting and crystallisation behaviours of the blends were analysed by differential scanning calorimetry (DSC). These results showed that the melting and crystallisation behaviours of PA12 were not significantly affected by blending with rubbers. It was also observed that the functional group present in the rubber phase has little effect on the melting and crystallisation behaviours of PA12.

Keywords: Thermal properties; Crystallisation behaviour; Activation energy

1. Introduction

Thermal and crystallisation behaviours of polymers and polymer blends are very relevant to the potential use of these materials in many demanding engineering applications. Thermal properties are important because of the fact that a study of stability of polymeric materials towards thermal degradation is one of the important criteria for designing these materials for engineering applications. Aliphatic polyamides (PAs) such as PA6, PA12, etc. are used in many demanding applications where the properties of thermal stability and fire resistance are priorities [1] and therefore have been extensively studied [2–4]. On the other hand, the mechanical and physical properties are influenced by the process of crystallisation during processing.

Polymer blending has been reported to have a great impact on the thermal stability [5–10] as well as crystallisation behaviour [11–17] of polymers. Varughese [5] reported that the blending of epoxidised natural rubber (ENR) with poly vinyl chloride (PVC) reduced the rate of HCl elimination in the first degradation step of PVC. The blending of a polymer with other polymers has stabilising as well as destabilising effects. Grassie [6] reviewed the stabilising effects of blending.

The incorporation of a second component to a crystallising polymer may lead to the following modifications in its crystallisation behaviour: (a) no effect on crystallisation rate or morphology, (b) retardation of crystallisation with or without change in morphology, (c) prevention of crystallisation at high loadings, and (d) acceleration of normally non-crystallising

* Corresponding author. Tel.: +91 481 2730003; fax: +91 481 2731002.
E-mail addresses: sabut552001@yahoo.com, sabut@sancharnet.in (S. Thomas).

0032-3861/$ - see front matter © 2006 Elsevier Ltd. All rights reserved.
doi:10.1016/j.polymer.2006.07.002

polymer as a result of induced mobility. George et al. [12] have studied the crystallisation behaviour of polypropylene/nitrile rubber (PP/NBR) blends and reported that the crystallinity of PP is affected by the addition of NBR. Moly et al. [17] have studied the thermal and crystallisation behaviours of linear low density polyethylene/poly(ethylene-*co*-vinyl acetate) (LLDPE/EVA) blends and found that the incorporation of EVA reduced the crystallinity of LLDPE phase in the blends.

PA12, the lowest water absorbing PA, is associated with excellent resistance towards solvents, abrasion, fatigue and environmental stress cracking and high processability. Styrene–ethylene/butylene–styrene (SEBS) is a triblock (A–B–A) thermoplastic elastomer which combines the processability of PS and elastomer property of poly (ethylene/butylene). It has been well demonstrated that incorporation of rubbers, especially functionalised rubbers, into PAs appreciably improves their low temperature toughness [18–24]. By the process of blending PA12 with rubbers, one can produce super-tough engineering thermoplastic elastomers which combine the excellent processability and elastomeric nature [25]. Meanwhile one can expect appreciable changes in the thermal and crystallisation behaviours of PA12 by the incorporation of amorphous rubbers. However, the thermal and crystallisation behaviours of the component polymers in the blend are influenced by their relative amount, chemical compatibility and the level of dispersion achieved in the compounding process. Several researchers have shown that miscibility/compatibility between two components in a binary blend is one of the decisive factors that determines the thermal stability of polymer blends [26–29].

In the present study we report on the effect of addition of SEBS rubbers on the thermal and crystallisation behaviours of PA12. Thermal stability and degradation kinetics have been studied by thermo gravimetric method. DSC has been employed to determine the melting and crystallisation behaviours of the blends. Specific attention has been paid to analyse the effect of functional group present in rubber phase on the thermal and crystallisation behaviours. It has been revealed from our previous studies that functional group present in rubber phase has profound effect on the mechanical properties and morphology of these blends [30]. Therefore, it is very important to correlate thermal and crystallisation behaviours of the blends in the presence and absence of functional group on rubber phase to the morphology and phase structure of the blends derived from scanning electron microscopic studies and dynamic mechanical thermal analysis, respectively.

2. Experimental

2.1. Materials

PA12 used in the present study (Vestamid L 1670), having a melt volume-flow rate (MVR) of 60 cm^3/10 min (at 250 °C/2.16 kg) and a density of 1.01 g/cm^3 was kindly supplied by Degussa High Performance Polymers, Marl, Germany. SEBS (Kraton G-1652E) with a melt flow index (MFI) 1 dg/min (200 °C/5 kg) and SEBS-*g*-MA with 1.84 wt% MA graft ratio (Kraton FG-1901X) having an MFI 20 dg/min (270 °C/5 kg) were obtained by the courtesy of Shell Chemical Company, Houston, Texas, USA. Both rubbers have a specific gravity 0.91 g/cm^3, styrene content 30 wt% and molecular weight of PS and poly (ethylene-*co*-butene) copolymer blocks ≈7000 and 37,500 g/mol, respectively.

2.2. Blend preparation

PA12 was dried in a vacuum oven at 80 °C for 24 h prior to blending. All the blends were prepared on a laboratory twin-screw extruder (Brabender DSE 25 with an L/D ratio of 22, Duisburg, Germany) equipped with necessary accessories. The barrel temperatures were maintained at 180, 190, 200 and 220 °C, respectively and the rotor speed was optimised as 40 rpm. The extruded blends were palletised using a home-made pelletiser. The extruded samples were dried again in a vacuum oven for 12 h before injection moulding. All the blends were injection moulded into dumb bell specimens of thickness 4 mm (according to ISO 3167) and film-gated plaques (80 mm × 80 mm) of 1 mm thickness in an injection moulding machine (Arburg 320 S 500-150). The mould and melting temperature ranges were maintained at 60 and 190–220 °C, respectively. The composition and code of the blend systems are presented in Table 1.

2.3. Morphology studies

The samples for phase morphology studies were cryogenically fractured in liquid nitrogen. The fractured surface was etched in toluene for 48 h for the extraction of the rubber phase. The etched surface was sputter coated with Au/Pd alloy in a sputter coating machine (Balzers SCD 050) for 150 s. A minimum of five photographs were taken for each sample using scanning electron microscope (SEM, Jeol 5400, Tokyo, Japan). About 200 particles were considered for morphological parameter measurements. The number (D_n) and weight (D_w) average diameters were determined by an automatic image analysing technique using the following equations:

The number average diameter,

$$D_n = \frac{\sum NiDi}{\sum Ni} \quad (1)$$

The weight average diameter,

$$D_w = \frac{\sum NiDi^2}{\sum NiDi} \quad (2)$$

Table 1
Compositions and codes of the samples used

Blends	PA12		SEBS		SEBS-*g*-MA	
	wt%	vol%	wt%	vol%	wt%	vol%
PS10	90	90.9	10	9.1	–	–
PS20	80	81.8	20	18.2	–	–
PS50	50	54.5	50	45.5	–	–
PM10	90	90.9	–	–	10	9.1
PM20	80	81.8	–	–	20	18.2
PM50	50	54.5	–	–	50	45.5

2.4. Thermo gravimetric analysis

The thermal degradation studies of the blends were done in a thermo gravimetric analyser (TGA), Mettler TG 50. The samples were scanned from room temperature to 600 °C at a heating rate of 20 °C/min. From the TG curve, the TG blind curve was subtracted.

2.5. Differential scanning calorimetry

The melting and crystallisation behaviours of the blends were determined using a Mettler 820 DSC thermal analyser. The first heating was done from room temperature to 200 °C at a rate of 40 °C/min followed by isothermal heating for 5 min and first cooling and second heating were performed at 10 °C/min in nitrogen atmosphere. The DSC thermal history of the samples is represented in Scheme 1.

2.6. Dynamic mechanical thermal analysis

The dynamic mechanical properties of the blends were analysed using a dynamic mechanical thermal analyser (Eplexor 150 N, Gabo Qualimeter, Ahlden, Germany) in tension mode. The static force and dynamic force were taken as 10 and ±5 N, respectively. Samples of 4 mm thickness and 10 mm width were used. The dynamic frequency was kept constant at 10 Hz and the heating rate was selected as 1 °C/min from −100 to +100 °C.

3. Results and discussion

3.1. Thermal stability of the blends

Thermal degradation temperature of PA12, and its blends with SEBS and SEBS-*g*-MA was determined using thermo gravimetric analysis. From the TG curves of PA12/SEBS (PS) and PA12/SEBS-*g*-MA (PM) blends presented in Figs. 1 and 2, weight losses at four selected temperatures (400, 420, 440 and 460 °C) and the temperature at maximum rate of degradation (T_{max}) were determined. The relative thermal stabilities of the polymers and their blends have been assessed from their integral procedural decomposition temperature (IPDT) proposed by Doyle [31].

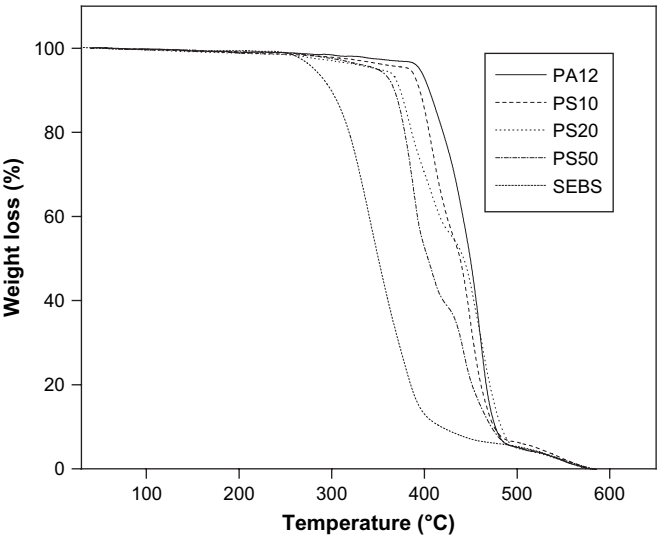

Fig. 1. Thermo gravimetric curves of PA12, SEBS and their blends.

Table 2 gives the % weight loss of the specimen remained at four selected temperatures viz. 400, 420, 440 and 460 °C. There is a gradual increase in weight loss in PS blends for a given composition, as temperature increases. At the same time as the wt% of rubber in the blends increases, a gradual increase in weight loss can be noticed (at 400 and 420 °C) indicating a decrease in thermal stability where as at 440 and 460 °C no regular trend is observed. A similar observation is found for PM blends, but interestingly, PM10 was found to possess better thermal stability compared to all other blends and to virgin PA12 at 400 and 420 °C. Further, it should be emphasized that the weight loss at all selected temperatures for blends with 20 wt% functionalised rubber (PM20) is

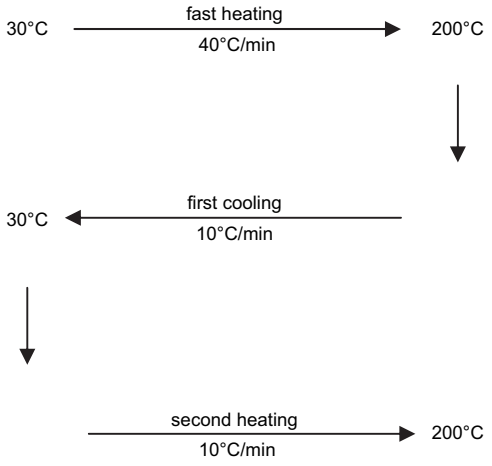

Scheme 1. DSC thermal history of samples.

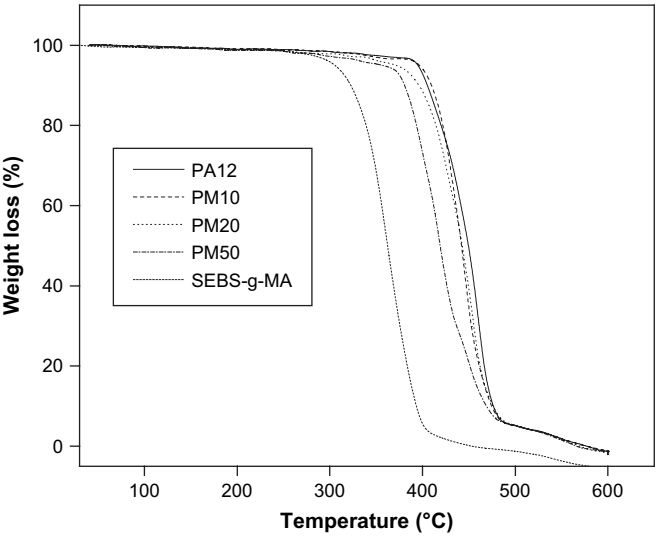

Fig. 2. Thermo gravimetric curves of PA12, SEBS-*g*-MA and their blends.

Table 2
Effect of blend ratio on weight losses at different temperatures in PS and PM blends

Blends	Weight loss at temperature (%)			
	400 °C	420 °C	440 °C	460 °C
PA12	6.9	19.9	38.2	67.6
PS10	14.1	36.8	50.8	79.4
PS20	29.6	41.9	48.4	67.7
PS50	47.5	60.1	69.6	84.7
PM10	5.7	17.6	45.6	79.1
PM20	11.3	24.6	45.7	78.5
PM50	26.8	51.8	71.9	85.9

even less than that for blends with 10 wt% unfunctionalised rubber (PS10). Thus, it is plainly clear from the figures and table that all blends with functionalised rubber (PM blends) are thermally more stable compared to those containing unmodified rubber (PS blends).

The temperature at maximum rate of degradation (T_{max}) and integral procedural decomposition temperature (IPDT) of PS and PM blends are given in Table 3. IPDT has been employed to evaluate the relative thermal stability of blends under the procedural conditions. IPDT of the blends was measured using Doyle's method [31] given as:

$$\mathrm{IPDT} = A^* K^* \left(T_f - T_i\right) - T_i \tag{3}$$

where T_i and T_f are the initial and final experimental temperatures, respectively, A^* is the ratio of area under the curve (A_1) and the total area ($A_1 + A_2$) of the thermogram and K^* is the coefficient of A^*. The T_{max} and IPDT of PA12 were found to be 733 and 716 K, respectively while those of SEBS and SEBS-*g*-MA were 617, 543 and 633, 550 K, respectively. From the table it can be seen that all PS blends exhibit two T_{max} corresponding to degradation of PA12 and rubber phase, respectively, which is a direct indication of high immiscibility and incompatibility of these blends. The T_{max} corresponding to the degradation of PA12 in PS blends is lower than that of virgin PA12 except in PS20 blend which interestingly, showed a slightly higher T_{max}. It is important to note that T_{max} corresponding to the degradation of SEBS rubber in the blends is higher than that of the virgin SEBS. PS20 and PS50 blends show almost the same T_{max} (which is 5–6% higher than that of virgin SEBS) corresponding to rubber phase while PS10 shows more than 10% increase in T_{max}. From the T_{max} values, one can claim that the thermal stability of PA12 decreases only slightly by the addition of rubber up to 20 wt% while in PS50, there is a notable decrease in thermal stability. However, in all the blends, thermal stability of the rubber phase increased appreciably. However, IPDT suggests that the thermal stability of PS blends decreased gradually with an increase in the amount of rubber in the blends. On the other hand, it is important to note that in PM blends only PM50 showed two T_{max}. This is interesting and can be taken as a direct indication of better compatibility associated with PM blends compared to PS blends. Note that T_{max} of PA12 initially decreases (PM10) and then increases. The T_{max} of rubber phase in PM50 is considerably greater than that of virgin SEBS-*g*-MA indicating an improvement in the thermal stability of rubber phase on blending. From IPDT it can be stated that addition of up to 20 wt% maleated rubber does not change the thermal stability of the blends.

Table 3
Effect of blend ratio on T_{max} and IPDT of polymer degradation in PS and PM blends

Blends	T_{max} (K)		IPDT (K)
PA12	733		716
PS10	724	680	709
PS20	735	655	704
PS50	716	659	688
SEBS	617		543
PM10	717		715
PM20	725		712
PM50	726	691	705
SEBS-*g*-MA	633		550

In short, the thermo gravimetric studies showed that PS blends are thermally less stable than PM blends. As the concentration of the rubber phase in the blend increases, the thermal stability of the blends decreases. In addition, in terms of thermal degradation properties, it can be predicted that PM blends are much more compatible than PS blends.

3.2. Kinetic analysis of thermal decomposition

Kinetic parameters such as pre-exponential factor (A), activation energy (E) and rate constant (k) for the thermal decomposition of PA12 in virgin form and in blends have been determined using different methods. Activation energy for the decomposition of PA12 in both PS and PM blends was measured using Coats–Redfern (CR) method [32].

In the CR method, both E and A were determined using the equation:

$$\ln\left[\frac{g(\alpha)}{T^2}\right] = \ln\{(AR/\Phi E)(1 - 2RT/E)\} - \frac{E}{RT} \tag{4}$$

where

$$g(\alpha) = \left\{\frac{1-(1-\alpha)^{1-n}}{(1-n)}\right\} \text{ for } (n \neq 1)$$

and

$$g(\alpha) = -\ln(1-\alpha) \text{ for } (n = 1)$$

The order of decomposition reaction was determined from the best linear fit of the kinetic curve that gives the maximum correlation coefficient. E and A are determined from the plot of $\ln[(g(\alpha)/T^2)]$ against the reciprocal of absolute temperature ($1/T$). From the slope of the curve E and from the intercept, the value of A can be calculated.

Finally, A and E were used to compute the rate constants for the thermal decomposition of PA12 in virgin form and in the blends using Arrhenius equation:

$$k = Ae^{-E/RT} \tag{5}$$

Table 4
Effect of blend ratio on the kinetic parameters of degradation of polymers in PS and PM blends

Blends	T_{max} (K)		Activation energy (kJ/mol)		ln A		Rate constant (s^{-1})	
PA12	733		180.4		29.49		0.90	
PS10	724	680	167.0	234.9	27.56	40.29	0.83	0.30
PS20	735	655	133.0	203.6	21.41	35.74	0.70	0.19
PS50	716	659	118.0	225.2	18.08	40.27	0.66	0.43
SEBS	617		146.2		16.53		0.315	
PM10	717		225.3		37.57		0.80	
PM20	725		187.9		31.03		0.86	
PM50	726	691	115.2	162.6	13.44	27.70	0.62	0.53
SEBS-*g*-MA	633		141.5		26.16		26.27	

The activation energy of degradation of PA12 in PS and PM blends is listed in Table 4. E of PA12 was found to be ~180 kJ/mol. Addition of rubber phase in PA12 decreases the E of PA12 in both PS and PM blends. However, it is important to note that the E of PA12 is greater in PM blends than in PS blends except for blends with 50% rubber. Greater value of E indicates greater thermal stability. It is interesting to note that both PM10 and PM20 showed much greater E values (even greater than that of PA12) than expected. However, this can be due to the fact that in both cases, due to only one T_{max} in the blend, the E obtained may be the sum of the E values of PA12 and SEBS-*g*-MA. Note that the E values in both blends (225 and 188 kJ/mol, respectively) are slightly greater than the arithmetic mean of the E values of PA12 and SEBS in corresponding PA12/SEBS blends (201 and 168 kJ/mol, respectively). Further, the greater E values for SEBS phase in PS blends are accounted for the lower T_{max} of SEBS.

It is also obvious from the table that all the PS blends exhibit two values for pre-exponential factor (A) corresponding to that of PA12 and SEBS. Note that in all blends A values are greater than that of corresponding virgin polymers. However, there is no trend in these values. On the other hand, among PM blends, only PM50 shows two A values. The rate

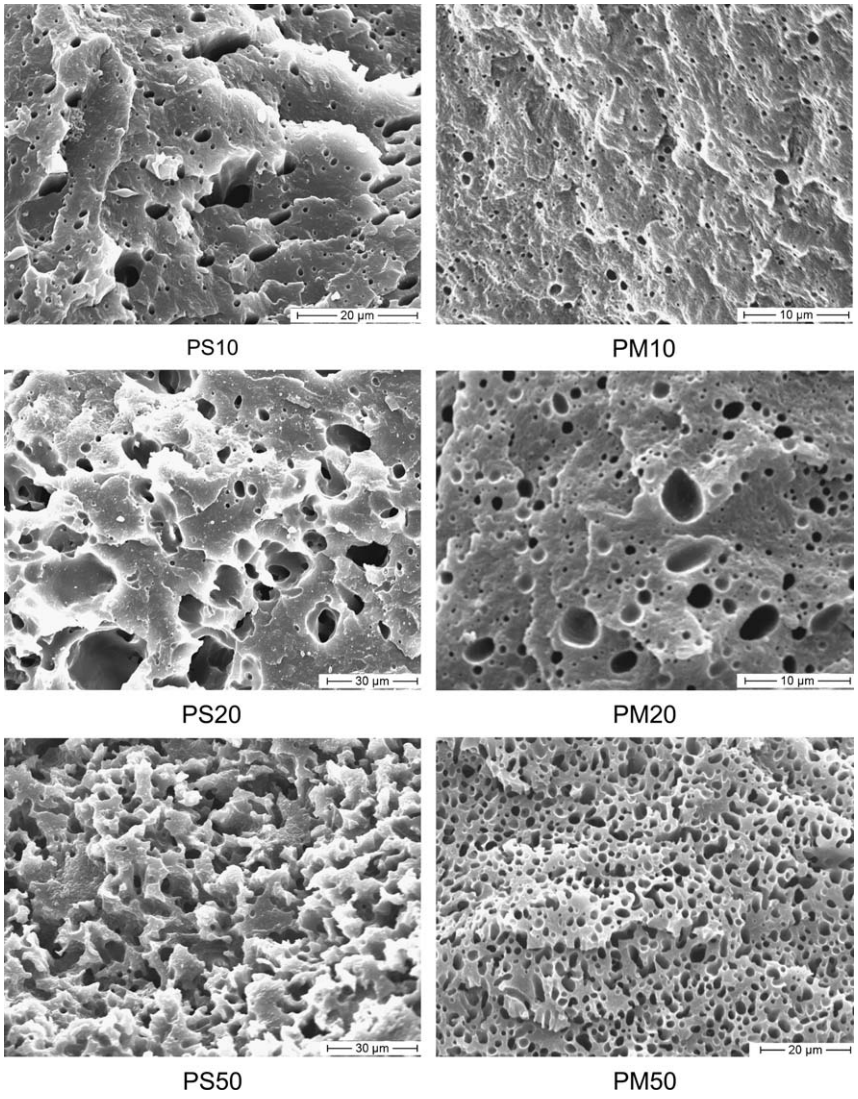

Fig. 3. SEM micrographs of PA12/SEBS and PA12/SEBS-*g*-MA blends.

constant for the degradation process of PA12 has been found to be 0.9 s^{-1}. There is no appreciable change in the rate constant of the degradation of PA12 in PS10 and PM10 blends. However, the rate of total degradation is significantly greater in the PS blend indicating relatively fast degradation in these blends. Note that the rate constant for the complete degradation is taken as the sum of the rate constants corresponding to individual phases in the blend. There is no appreciable change in rate constants of degradation of PS20 and PM20 blends also. Among the blends, the degradation process is faster in blends with 50 wt% rubber phase i.e., PS50 and PM50, even though the rate constant of PA12 in both blends is relatively low. Thus, it can be concluded that there is no considerable change in the rate of degradation of blends upon addition of 20 wt% rubber, but beyond that the degradation process becomes faster.

It is important to note that there is a strong link between the thermal properties and morphology of the blends. The morphological parameters of PS and PM blends derived from SEM micrographs shown in Fig. 3 are presented in Table 5. It can be realised from the table that PM blends exhibit a more fine, uniform and stable phase morphology compared to PS blends. This is attributed to the interfacial chemical reaction between the maleic anhydride group present in SEBS-*g*-MA and amine group present in PA12 leading to the formation of a copolymer, which could act as a compatibiliser. The in situ formed compatibiliser in PM blends decreases the interfacial tension and suppresses the coalescence rate and thereby stabilises the morphology. Thus, the interfacial situation is improved resulting in a better compatibility in PM blends. A detailed discussion is given elsewhere [30]. It has been revealed from this study that this stabilisation of morphology through chemical reaction has a profound effect on the thermal properties of the blends. All the thermal properties revealed that PM blends, which possess more stable phase morphology, are thermally more stable compared to the corresponding PS blends as predicted by the morphology parameters. In blends with 10 and 20 wt% rubber, the rubber phase forms the dispersed phase. In PM blends the better compatibility at the interface decreases the unfavourable interfacial interactions between the PA and rubber phases and thereby the PA matrix decreases the rate of degradation of the rubber. On the other hand, in PS10 and PS20 blends, even though the rubber phase is dispersed in PA matrix, the strong unfavourable interactions between the matrix and the dispersed phases tend to prevent the matrix phase to protect the dispersed rubber phase from degradation. Further, in PS50, which possesses a co-continuous morphology, the rubber phase is continuous and therefore more prone to degradation compared to PM50 blend in which rubber forms the dispersed phase.

In addition, both morphology and DMTA (presented in Figs. 4 and 5) suggest a two-phase structure for PS20, PM20, PS50 and PM50. From Fig. 5, which shows the effect of blend ratio on the tan δ of neat polymers, one can see that the glass transition temperature (T_g) of virgin PA12 is at around 50 °C, and a peak corresponding to secondary relaxation of PA12 is at around −57 °C. The T_g of SEBS and SEBS-*g*-MA is found to be at −49 and −47 °C, respectively. Further, a part of the relaxation peak close to 100 °C in SEBS and SEBS-*g*-MA rubbers can be assigned to the PS blocks in them. All the blends show two peaks corresponding to the T_g of both PA12 and rubber phases. It should be noted that blending has no

Table 5
Morphological parameters of dispersed rubber phase in PA12/SEBS and PA12/SEBS-*g*-MA blends

Blends	$\bar{D}_n$(μm)	$\bar{D}_w$(μm)	$\bar{D}_w/\bar{D}_n$
PS10	1.17	1.56	1.33
PS20	5.03	7.71	1.53
PM10	0.63	0.89	1.41
PM20	0.87	1.38	1.59
PM50	1.63	2.08	1.28

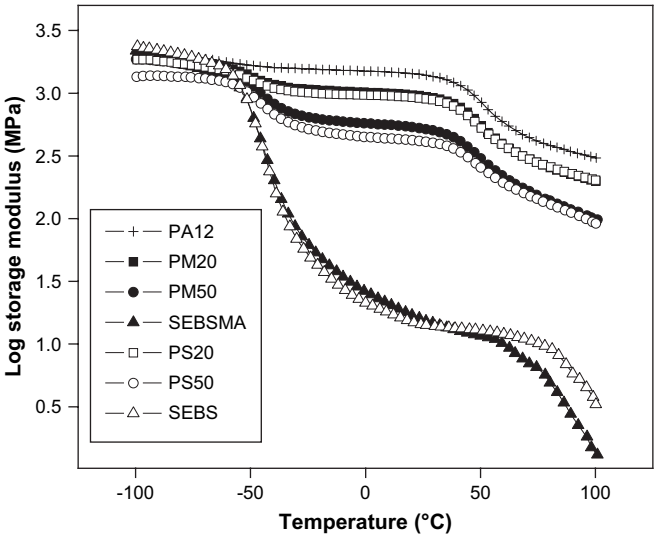

Fig. 4. Variation of storage modulus of PA12 blends with SEBS and SEBS-*g*-MA rubbers as a function of temperature.

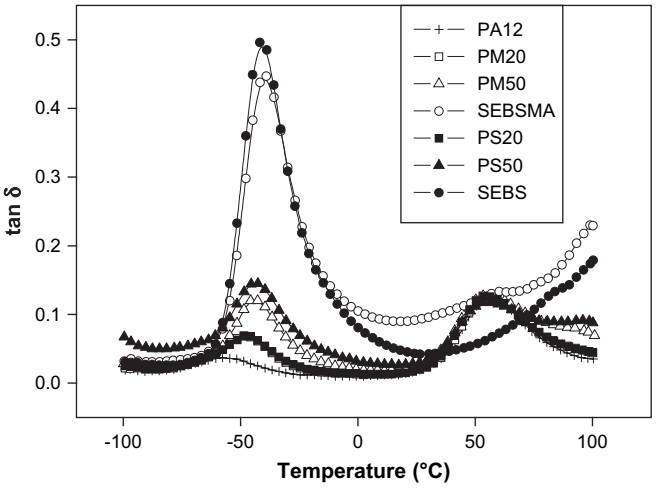

Fig. 5. Variation of tan δ of PA12 blends with SEBS and SEBS-*g*-MA as a function of temperature.

appreciable effect on the T_g of PA12, SEBS and SEBS-*g*-MA. Interestingly, the peak corresponding to PS block cannot be resolved in the blends. This is also found to be true from thermal analysis as far as PS20, PS50 and PM50 (which show multiple decomposition peaks) are concerned while PM20 possesses only one T_{max}. This may be due to the less sensitivity of thermal analysis method compared to others. However, there is still some uncertainty and detailed investigation is needed.

3.3. Melting and crystallisation behaviours of blends

The heating and cooling curves of PA12 and its blends with SEBS and SEBS-*g*-MA are given in Figs. 6–9. The effects of addition of SEBS and SEBS-*g*-MA on the melting and crystallisation behaviours of PA12 are summarised in Table 6. The important parameters which can be obtained from the table include:

a. crystallisation temperature (T_c),
b. melting point (T_m),
c. normalised enthalpy of crystallisation (ΔH_c),
d. normalised enthalpy of fusion (ΔH_f), and
e. percentage crystallinity.

Percentage crystallinity of component polymers in the blend is obtained from the expression:

$$\%\ \text{Crystallinity} = \left(\Delta H_f / \Delta H_f^0\right) 100 \tag{6}$$

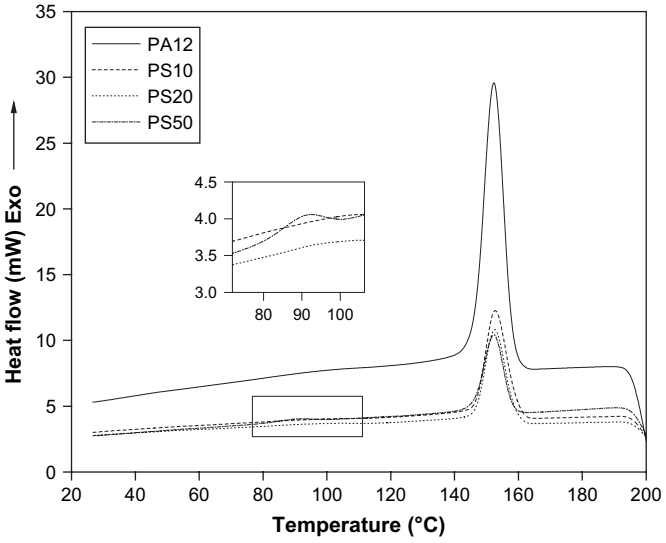

Fig. 6. Effect of blend ratio on DSC cooling curves of PA12 in PA12/SEBS blends.

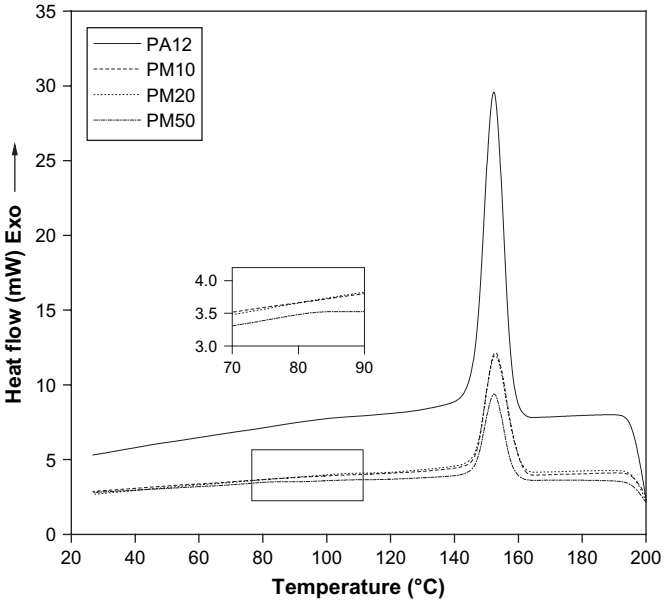

Fig. 7. Effect of blend ratio on DSC cooling curves of PA12 in PA12/SEBS-*g*-MA blends.

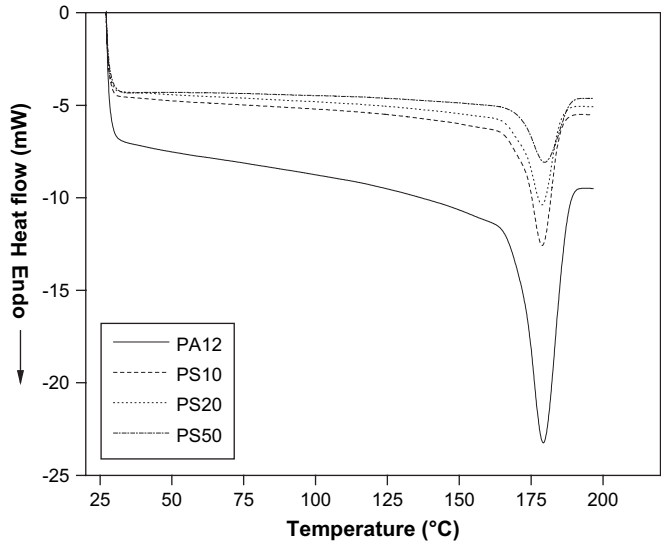

Fig. 8. Effect of blend ratio on DSC cooling curves of PA12 in PA12/SEBS-*g*-MA blends.

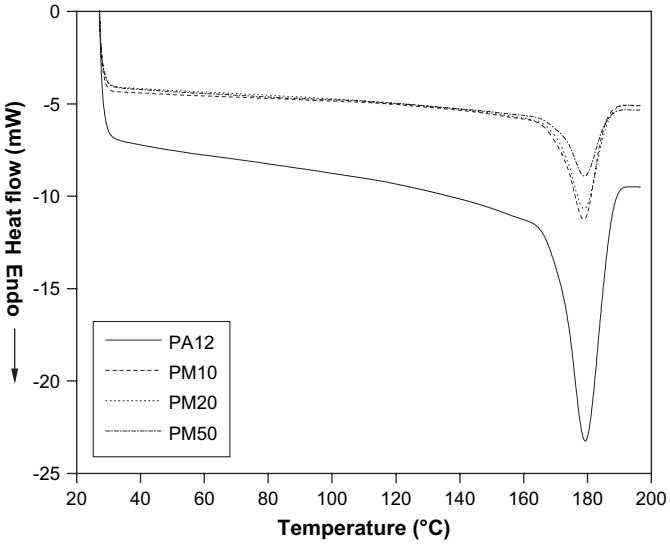

Fig. 9. Effect of blend ratio on DSC heating curves of PA12 in PA12/SEBS-*g*-MA blends.

Table 6
Effect of addition of rubber on the melting and crystallization behaviours of PA12

Blends	T_c (°C)	T_m (°C)	ΔH_c (J/g) normalised	ΔH_f (J/g) normalised	Crystallinity (%)
PA12	155	179	65.7	66.6	70
PS10	155	179	65.8	65.6	69
PS20	155	179	67.0	65.1	69
PS50	153	181	55.4	63.8	67
PM10	155	179	66.4	65.3	69
PM20	155	179	63.6	63.6	67
PM50	154	179	69.8	61	64

where ΔH_f is the enthalpy of fusion obtained calorimetrically and ΔH_f^0 is the enthalpy of fusion of the 100% crystalline PA12. ΔH_f^0 of PA12 was taken as 95 J/g.

The T_c, T_m and percentage crystallinity of PA12 were observed as 155, 179 °C and 70%, respectively. It is obvious from Table 6 that the crystallisation temperature and melting point of PA12 remained unchanged by the addition of rubber. There is no considerable change in the normalised values of ΔH_c and ΔH_f of PA12 on blending with SEBS rubber (with in the limit of 5%) except for ΔH_c of PS50. It showed more than 15% difference with the ΔH_c of virgin PA12. However, this may be due to the incomplete crystallisation of PA12 in PS50 which is evident from an additional crystallisation peak at ~92 °C observed in the cooling curve of PS50 blend. From the table, it can be seen that the presence of up to 20 wt% SEBS-*g*-MA did not affect the melting and crystallisation behaviours of PA12. However, it is seen that ΔH_f of PA12 is affected in PM50. This observation offers an apparent conflict with the ΔH_c of PA12, which registered a marginal increase in PM50. It is interesting to note that the additional crystallisation peak of PA12 that observed ~92 °C in PS50 blend is not seen in PM50. Additionally, the % crystallinity values of PA12 in blends reveal that the presence of rubber phase has no considerable effect on the crystallisation behaviour of the blends.

Thus, from the melting and crystallisation behaviours of PA12 in PS and PM blends it can be concluded, in general, that the presence of rubber did not affect the overall crystallisation kinetics. Moreover, attention should be paid to the fact that the presence of functional group on rubber phase has no appreciable influence on the melting and crystallisation behaviours of PA12. However, this is only a qualitative inference and the present investigation is not adequate to predict the complete crystallisation behaviour of the blends. On the basis of morphology and thermal properties of the blends one can state that PM blends are more compatible than PS blends as the interfacial chemical reaction increases the favourable interfacial interactions. Thus, a change in melting and crystallisation behaviours in the presence of functional group in rubber phase can be expected. However, this is overruled by the experimental results on crystallisation behaviour. The plausible explanation for this observation is that the interfacial chemical reactions in the present system usually occur at the amorphous phase and, therefore, will not contribute appreciable change in its crystallisation behaviour.

4. Conclusions

From the present study, which is devoted to investigate the thermal properties of PA12/SEBS and PA12/SEBS-*g*-MA blends, the following conclusions can be drawn.

1. Addition of rubber up to 20 wt% did not affect the thermal stability of PA12 appreciably. However, addition of 50% rubber marginally decreased the thermal stability of the blends.
2. PA12/SEBS-*g*-MA blends out performed PA12/SEBS blends in terms of thermal stability suggesting that presence of functional group has a great impact on the thermal stability of the blends. The greater thermal stability of the blends with functionalised rubber is directly attributed from the better morphological stability of the blends.
3. Kinetic parameters of degradation showed that the activation energy of degradation of PA12 in PA12/SEBS-*g*-MA blends was greater than that in the corresponding PA12/SEBS blends. On the other hand, there was no significant difference between the rate constant for degradation of PA12 in both blends.
4. A strong link between the morphology and thermal properties of the blends was evaluated from the studies. The superior thermal stability of PA12/SEBS-*g*-MA blends compared to that of PA12/SEBS blends was found to be due to the formation of copolymer by interfacial chemical reactions during processing in PA12/SEBS-*g*-MA blends which acted as compatibiliser.
5. Crystallinity of the blends is little affected by the presence of rubber phase in the blend. There was no considerable difference between PS and PM blends in terms of their crystallisation behaviour.

References

[1] Williams IG. Plast Today 1984;19:14.
[2] David C. In: Bawford CH, Tipper CFH, editors. Comprehensive chemical kinetics: degradation of polymers, vol. 14. Amsterdam: Elsevier; 1975.
[3] Bhuiyan AL. Polymer 1984;25:1699.
[4] Levchik SV, Weil ED, Lewin M. Polym Int 1999;48:532.
[5] Varughese KT. Kaustschuk Gumi Kunststoffe 1988;41:114.
[6] Grassie N, editor. Developments in polymer degradation. London: Applied Science; 1998.
[7] Varghese H, Bhagavan SS, Thomas S. J Therm Anal Calorim 2001;63:749.
[8] Varghese H, Johnson T, Bhagavan SS, Joseph S, Thomas S, Groeninckx G. J Polym Sci B Polym Phys 2002;40:1556.
[9] Stack S, O'Donogbue O, Birkinshaw C. Polym Degrad Stab 2003;79:29.
[10] Vrandečić NS, Klarić I, Kovačić T. Polym Degrad Stab 2004;84:23.
[11] Kozhy AT, Kuriakose B, Thomas S, Varghese S. Polymer 1993;34:2438.
[12] George S, Varughese KT, Thomas S. Polymer 2000;41:5485.
[13] Jang GS, Cho WJ, Ha CS. J Polym Sci B Polym Phys 2001;39:1001.
[14] Dutt G, Kit KM. J Appl Polym Sci 2003;87:1984.
[15] Rocco AM, Bielschowsky CE, Pereira RP. Polymer 2003;44:361.
[16] Dangseeyn N, Supaphol P, Nithitanakul M. Polym Test 2004;23:187.
[17] Moly KA, Radusch HJ, Androsh R, Bhagavan SS, Thomas S. Eur Polym J 2005;41:1410.
[18] Dijkstra K, Gaymans RJ. Polymer 1994;35:332.
[19] Kelnar M, Stephan L, Jakisch L, Fortelny I. J Appl Polym Sci 1999; 74:1404.
[20] Chen H, Yang B, Zang H. J Appl Polym Sci 2000;77:928.

[21] Oderkerk J, de Schaetzen G, Goderis B, Hellemans L, Groeninckx G. Macromolecules 2002;35:6623.
[22] Bai SL, Wang GT, Hiver JM, G'Sell C. Polymer 2004;45:3063.
[23] Huang JJ, Keskkula H, Paul DR. Polymer 2004;45:4203.
[24] Bhattacharyya AR, Ghosh AK, Misra A, Eichhorn K-J. Polymer 2005; 46:1661.
[25] Leibler L. Prog Polym Sci 2005;30:898.
[26] Santra RN, Mukundo PG, Chaki TK, Nando GB. Thermochim Acta 1993;219:283.
[27] Lizymol PP, Thomas S. Polym Degrad Stab 1993;41:59.
[28] Asaletha R, Kumaran MG, Thomas S. Polym Degrad Stab 1998; 61:431.
[29] Oommen Z, Groeninckx G, Thomas S. J Polym Sci B Polym Phys 2000; 38:525.
[30] Jose S, Thomas S, Lievana E, Karger Kocsis J. J Appl Polym Sci 2005; 95:1376.
[31] Doyle CD. Anal Chem 1961;33:77.
[32] Coats AW, Redfern JP. Nature 1964;201:68.